Native iron in Miocene sediments

D. M. Pechersky,[1] D. K. Nurgaliev,[2] and V. M. Trubikhin[3]

Received 19 July 2008; accepted 22 August 2008; published 14 September 2008.

[1] With the aid of thermomagnetic analysis up to 800°C we studied the detailed pattern of how native iron is distributed in Miocene sediments of two sections, Khalats (Turkmenia) and Kvirinaki (Georgia), which are more than 1500 km apart. Out main result is that enrichment by native iron particles was synchronous in both sections. This phenomenon is of extraterrestrial origin and does not depend upon local conditions of deposition. The length of iron-enriched interval (from 12.6 to 12.2 Ma) over a vast area cannot result from a single impact event. *INDEX TERMS:* 1029 Geochemistry: Composition of aerosols and dust particles; 1512 Geomagnetism and Paleomagnetism: Environmental magnetism; 1594 Geomagnetism and Paleomagnetism: Instruments and techniques; 2129 Interplanetary Physics: Interplanetary dust; *KEYWORDS:* cosmic metallic iron, sediments, themomagnetic analysis, Curie point.

Citation: Pechersky, D. M., D. K. Nurgaliev, and V. M. Trubikhin (2008), Native iron in Miocene sediments, *Russ. J. Earth. Sci., 10,* ES6004, doi:10.2205/2008ES000306.

In memory of our friend and colleague Boris Vladimirovich Burov

Introduction

[2] According to numerous data, the particles of metallic (native) iron and nickel are common on the Earth surface, but their temporal distribution is very poorly studied. Unfortunately, thermomagnetic analysis (TMA) of sediments had not been used for this purpose. Recently, TMA up to 800°C was employed during petromagnetic (rock-magnetic) studies of sediments at the K/T boundary [*Grachev et al.,* 2005; *Molostovsky et al.,* 2006; *Pechersky et al.,* 2006a, 2006b]; (D. M. Pechersky et al., in press, 2008a,b). As a result, it has been found that metallic iron in low concentration, usually below 0.001%, is widespread in sediments [*Pechersky,* 2008a, 2008b]. No enrichment by metallic iron was found close to the K/T boundary. A possible influence of oxidation of iron particles and their re-deposition has led to an idea that it is worth studying how iron particles are distributed in younger sediments, of Miocene and Pliocene ages; however, we abstained from investigating present-day sediments, which may be contaminated by anthropogenic input. The Khalats (Turkmenia) and Kvirinaki (Georgia) sections were selected for such studies as both have already been sampled. These sections satisfy main provisions for such studies, which run as follows: they are about 1500 km apart, local factors, including possible oxidation of iron particles and their re-deposition, can be ruled out; the sediments accumulated in very different physical-geographic environment; the sediments contain abundant fossils for reliable biostratigraphic dating; magnetostratigraphical information is available for both sections (Tables 1 and 2). The Khalats section comprises continental sediments, mostly cobble conglomerates with lenses of sand, sandstone and sandy siltstone. Fine-grained varieties were sampled for paleo- and petromagnetic studies. According to biostratigraphic data, this section represents a nearly continuous succession of Middle Miocene and early Late Miocene age, from the upper part of the Sakaraul-Kotsakhurian stage to the late Sarmatian stage (Table 1). Correlation of paleomagnetic data with the magnetochronostratigraphic scale of *Berggren et al.* [1995] showed that the Khalats section includes magnetic chrons from C5Cn to C4Ar, which corresponds to the age interval from 16.5 to 9.5 Ma (Table 1). In contrast to the Khalats sections, the Kvirinaki section is composed of marine terrigenous sediments with noticeable carbonate content. According to biostratigraphic data, this section encompasses a large part of the Middle and Late Miocene, from the Tarkhanian stage to the Middle Sarmatian stage, with a large hiatus between the Chokrakian and Karaganian stages (Table 2). Correlation of paleomagnetic data with the magnetochronostratigraphic scale of *Berggren et al.* [1995] showed that the Kvirinaki section includes magnetic chrons from C5Br to

[1]Schmidt Institute of Physics of the Earth, Russian Academy of Sciences, Moscow, Russia
[2]Geological Faculty, Kazan State University, Kazan, Tatarstan, Russia
[3]Geological Institute, Russian Academy of Sciences, Moscow, Russia

ISSN: 1681–1208 (online)

Table 1. The position in the section and age of samples, Halats

Sample, no.	meters	stage	chron	age, Ma
67-68-I	60	Akchagilian	Gauss	2.7
68-68-I	73		”	2.85
66-68-I	95		”	2.95
65-68-2	108		”	3
64-68-II	119		”	3.06
63-68-II	126		”	3.12
62-68-II	145		”	3.25
interruption				
59-68-3	220	Upper Sarmatian	C4Ar	9.5
58-68-II	242	”	”	9.7
57-68-II	245	”	”	9.9
56-68-II	276	Middle Sarmatian	C5n	10
55-68-II	*306*	”	”	*10.2*
54-68-II	326	”	”	10.4
52-68-II	344	”	”	10.6
51-68-II	367	”	”	10.7
50-68-II	387	”	”	10.8
49-68-I	*417*	”	”	*10.95*
48-68-II	437	”	C5r	11.2
47-68-II	*468*	*Lower Sarmatian*	”	*11.5*
46-68-II	492	”	”	11.8
45-68-II	510	”	”	11.9
44-68-II	532	”	C5An	12
43-68-II	536	”	”	12.05
42-68-II	*557*	*Konkian*	”	*12.2*
41-68-II	*583*	”	”	*12.35*
39-68-III	*602*	*Karaganian*	*C5Ar*	*12.45*
38-68-I	*625*	*Tschokrakian*	”	*12.55*
37-68-I	643	Tarkhanian	”	12.65
36-68-I	646	”	”	12.66
35-68-I	670	”	”	12.85
34-2-68-I	692	”	C5ABn	13
33-68-I	722	”	”	13.5
32-68-II	752	”	C5ABr	13.65
31-68-I	783	”	C5ACn	13.8
29-68-I	827	”	”	14.2
28-2-68-I	854	”	C5ADn	14.55
27-68-I	878	”	C5ADr	14.75
26-68-IV	906	”	C5Bn	15
25-68-I	*909*	”	”	*15.01*
24-68-I	*912*	”	”	*15.02*
23-68-I	*930*	”	*C5Br*	*15.2*
22-68-III	942	”	”	15.6
21-68-I	945	”	”	15.61
20-68-I	947	”	”	15.63
14-68-III	1007	Sakharauian-Kozahurian	C5Cn	16.2
16-68-I	1029	”	”	16.4
13-68-I	1042	”	”	16.5
11-68-I	1045	”	”	16.51

Note: The samples with metallic iron $\geq$0.001% are shown in italic.

C5n, which corresponds to the age interval from 15.9 to 10.2 Ma with the gap from 14.6 to 13.0 My (Table 2). Thus the sections cover similar intervals, which is very important for establishing the synchronism, or the lack thereof, of iron-enriched levels.

[3] This paper presents the results of magnetolithologic and magnetomineralogical study of the Khalats and Kvirinaki sections, the distribution of metallic iron particles being out primary goal.

Methods of Petromagnetic Studies

[4] Petromagnetic studies included measurements of sample magnetization and its dependence upon temperature, that is thermomagnetic anaysis (TMA) (Figure 1). TMA was performed with the aid of Curie express balance [*Burov et al.,* 1986], which allowed measuring the intensity of induction magnetization at different temperatures with heating rate of 100°/min. Because of high sensitivity of the equipment, very small samples of less than 0.2 g were used. TMA was performed in the constant magnetic field of 200 mT. The curves of $M_i(T)$ after the first and second runs to 800° were obtained for all samples.

[5] We estimated the content of goethite, magnetite and titanomagnetite combined (labeled magnetite+titanomagnetite or MT+TM hereafter), and metallic iron. (Some thermomagnetic parameters can be used to gain information about magnetite and titanomagnetite separately; in this particular case, however, we are not interested in this). To achieve this goal, the contribution of each mineral into M_i was determined using the $M_i(T)$ curves and, then, it was divided by the specific saturation magnetization of each mineral. M_s values of 90, 200, and 0.25 Am^2 kg^{-1} for magnetite+titanomagnetite, iron and goethite, respectively, were used.

[6] To estimate the relative contribution of the total iron content in a rock, we used the intensity of magnetization at 800°C (M_{800}), which is the sum of paramagnetic and diamagnetic magnetizations. For natural minerals, the former is by two or three orders of magnitude higher than the diamagnetic magnetization of quartz and calcite [*Rochette et al.,* 1992]. Hence the paramagnetic component strongly prevails in M_{800} values for sediments, except for almost purely diamagnetic rocks like limestone or quartz sandstone.

[7] We used the following indirect features for mineral identification: a) The growth of magnetization above 500°C (Figure 1a, Samples 399 and 402) indicates the presence of pyrite, which is oxidized to magnetite and hematite above 500°C [*Novakova and Gendler,* 1995]. b) The presence of Curie point around 580–600°C on the $M_i(T)$ curve and the decrease of magnetization and Curie temperature after the first heating points to decomposed titanomagnetite, which becomes partly homogenized during heating (Figure 1a, sample 24). c) The presence of Curie point at 260–300°C on the $M_i(T)$ curve and its lessening and magnetization growth (in contrast to titanomagnetite) after heating to 800°C point to antiferrimagnetic hemoilmenite of intermediate composition, which is the common product of het-

Table 2. The position in the section and age of samples, Kvirinaki

Sample, no.	meters	stage	chron	age, Ma	Sample, no.	meters	stage	chron	age, Ma
450	26	Middle Sarmatian	C5n	10.17	411	276	”	”	11.85
449	31	”	”	10.21	410	278	”	”	11.86
448	*40*	”	”	*10.27*	409	282	”	C5An	11.9
447	44	”	”	10.3	408	284	”	”	11.93
446	50	”	”	10.33	407	286	”	”	11.97
445	55	”	”	10.37	406	288	”	”	12
444	64	”	”	10.43	405	290	”	”	12.03
443	70	”	”	10.47	404	292	”	”	12.06
442	77	”	”	10.52	403	294	”	”	12.1
441	83	”	”	10.56	402	296	”	”	12.13
440	95	”	”	10.64	*401*	*298*	”	”	*12.16*
439	102	”	”	10.68	400	300	”	”	12.19
438	112	”	”	10.75	*399*	*304*	”	”	*12.26*
437	122	”	”	10.82	*398*	*308*	*Konkian*	”	*12.33*
436	*129*	”	”	*10.86*	397	310	”	”	12.36
435	138	”	C5r	10.92	396	312	”	”	12.39
434	146	”	”	10.98	*395*	*313*	*Karaganian*	”	*12.4*
433	156	”	”	11.05	*394*	*314*	”	”	*12.5*
432	166	”	”	11.11	*393*	*316*	”	*C5Ar*	*12.6*
431	174	”	”	11.17	392	318	”	”	12.8
430	180	”	”	11.21	391	320	”	”	13
429	188	”	”	11.26	interruption				
428	195	”	”	11.31	390	322	Tarkhanian-Tschokrakian	C5ADr	14.6
427	202	”	”	11.35	389	328		”	14.68
426	210	”	”	11,41	*386*	*344*	”	”	*14.9*
425	218	Lower Sarmatian	”	11.46	385	348	”	”	14.96
424	222	”	”	11.49	*384*	*354*	”	”	*15.04*
423	226	”	”	11.51	383	358	”	C5Bn	15.1
422	232	”	”	11.55	382	363	”	”	15.17
421	237	”	”	11.59	381	367	”	”	15.23
420	244	”	”	11.63	380	372	”	”	15.3
419	248	”	”	11.66	*379*	*378*	”	”	*15.38*
418	*255*	”	”	*11.71*	378	383	”	”	15.45
417	258	”	”	11.73	*377*	*387*	”	”	*15.51*
416	260	”	”	11.74	376	390	”	”	15.55
415	262	”	”	11.76	375	395	”	”	15.62
414	266	”	”	11.78	374	399	”	C5Br	15.68
413	270	”	”	11.81	373	403	”	”	15.75
412	273	”	”	11.83	371	410	”	”	15.85

Note: The samples with metallic iron ≥0.001% are shown in italic.

erophase oxidation of ilmenite; the latter mineral becomes partly homogenized above 800°C and is transformed into a ferrimagnetic state, which leads to the decrease of the Curie temperature and the growth of magnetization. It is possible that oxidation of paramagnetic ilmenite also results in formation of ferrimagnetic hemoilmenite of intermediate composition during TMA; consequently, a new magnetic phase with the Curie point about 250–300°C is created, and the intensity of sample magnetization grows up (Figure 1a, samples 24 and 402).

The Results of Petromagnetic Studies

[8] TMA shows that the following magnetic minerals are present in the sediments from the Khalats and Kvirinaki sections:

[9] 1) A magnetic phase with T_C = 90–150°C is present in most samples but disappears after the first heating; its share in M_i is 5–20%. This phase is likely to be weakly ferromagnetic Fe-hydroxides like goethite (Figures 2 and 3).

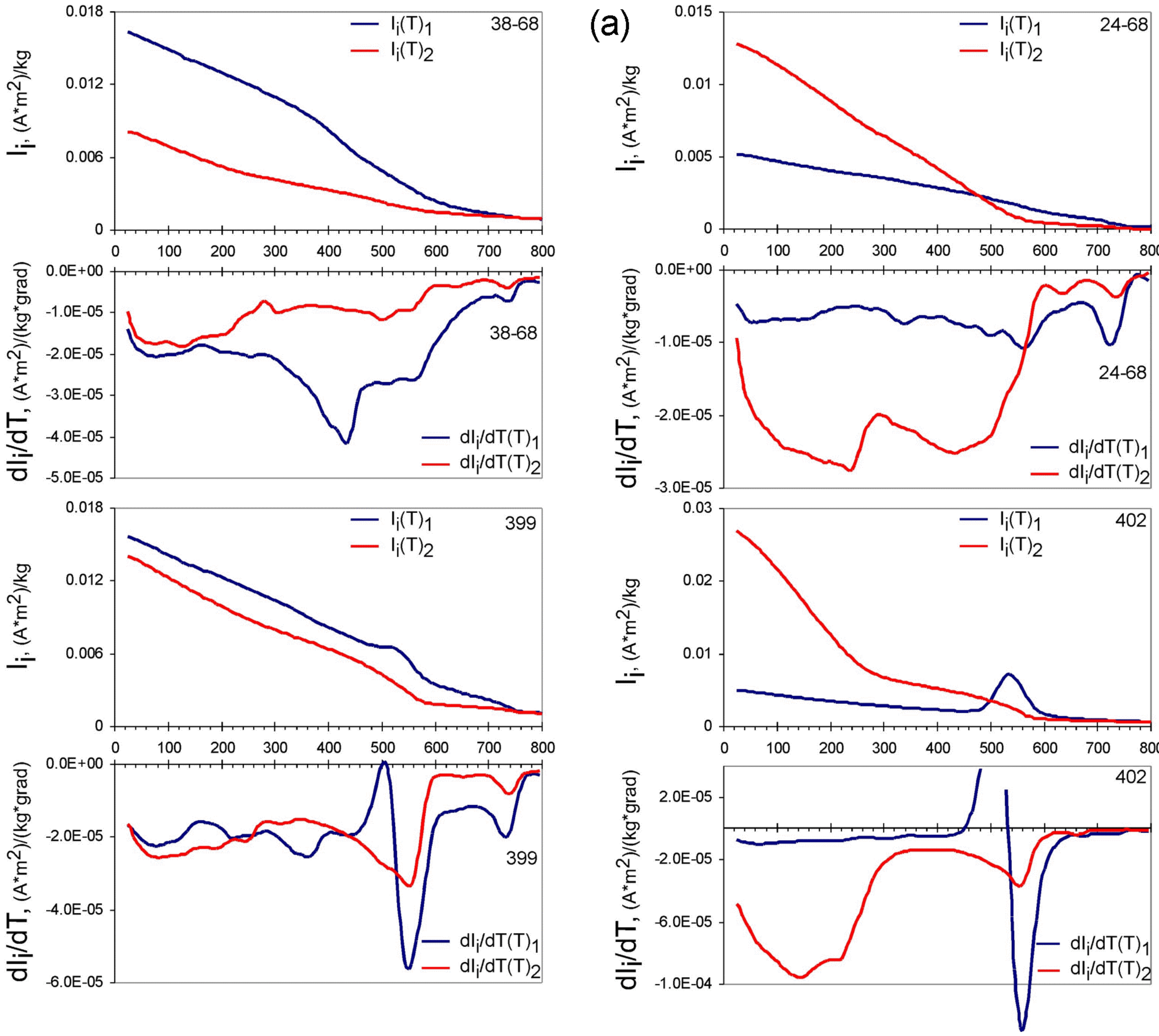

Figure 1. (a) The examples of TMA results. Numbers on the plots are sample numbers: 24 and 38 are from the Khalats section, 399 and 402 are from the Kvirinaki section. Note a peak related to transformation of pyrite to magnetite and hematite on the latter two.

[10] 2) A magnetic phase with T_C = 180–300°C that is present in many samples accounts for 0–40% of M_i. After heating to 800°C, the contribution of this phase often increases, while the Curie temperature decreases, which is typical for hemoilmenite of intermediate composition. During heating, this mineral becomes partly homogenized and/or ilmenite is transformed into hemoilmenite (Figure 1a, sample 402).

[11] 3) A magnetic phase with T_C = 200–370°C is found in most samples but disappears after heating to 300–400° (Figure 1a, sample 38); hence, as a rule, this is not a Curie temperature but the result of transformation of maghemite into hematite. Judging by considerable decrease of magnetization intensity after heating (M_t/M_o is often less than 0.5, Figures 2 and 3), a significant part of magnetite and titanomagnetite in the sediments of both sections is maghemitized.

[12] 4) A magnetic phase with T_C = 510–640°C is present in all studied samples from both sections (Figures 2 and 3); its contribution into M_i ranges from less than 5% to 90%. As a rule, this phase is preserved during heating, but its concentration usually decreases, while the Curie temperature either remains unchanged (magnetite) or shifts to lower values (titanomagnetite). After heating to 800°C, titanomagnetite grains become partly homogenized; the latter feature allows us to state that titanomagnetite is present in many samples. Below, the combined contribution of magnetite and titanomagnetite (MT+TM) is used for analysis.

[13] 5) A magnetic phase with T_C = 670–680°C is present in lower amount in some Khalats samples but is absent altogether in the Kvirinaki section. After heating to 800°C,

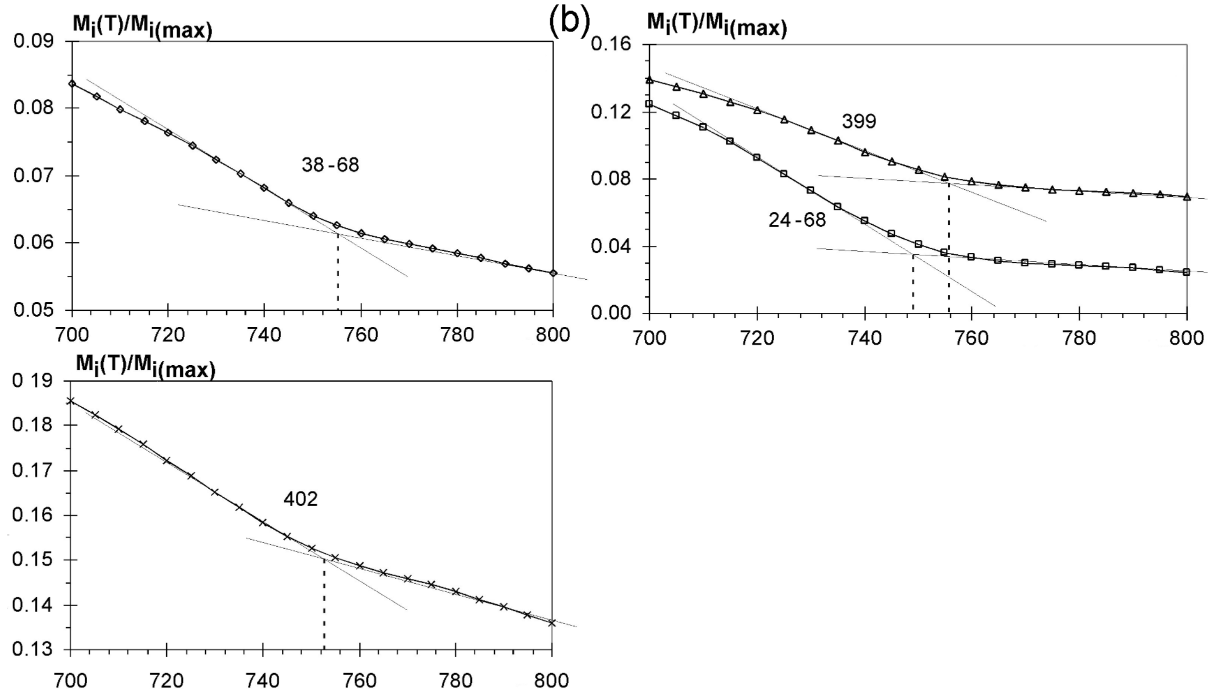

Figure 1. (b) The examples of TMA results. The 700–800°C interval TMA is highlighted to illustrate the Curie temperatures of metallic iron for the same samples as Figure 1a.

this phase appears in all pyrite-bearing samples as a result of pyrite oxidation at high temperatures. Very likely, it is hematite.

[14] 6) A magnetic phase with $T = 720$–$780°C$ (Figure 1b) is the main goal of this study. This is metallic iron with minor impurities. It is present in many samples, and its contribution into M_i ranges from 0 to 60% (Figures 2 and 3). This phase partly or completely oxidizes after heating to 800°C.

[15] 7) Above 500°C, magnetization of many Kvirinaki samples grows considerably, with a peak at 540°C (Figure 1a, samples 399 and 402). This indicates the presence

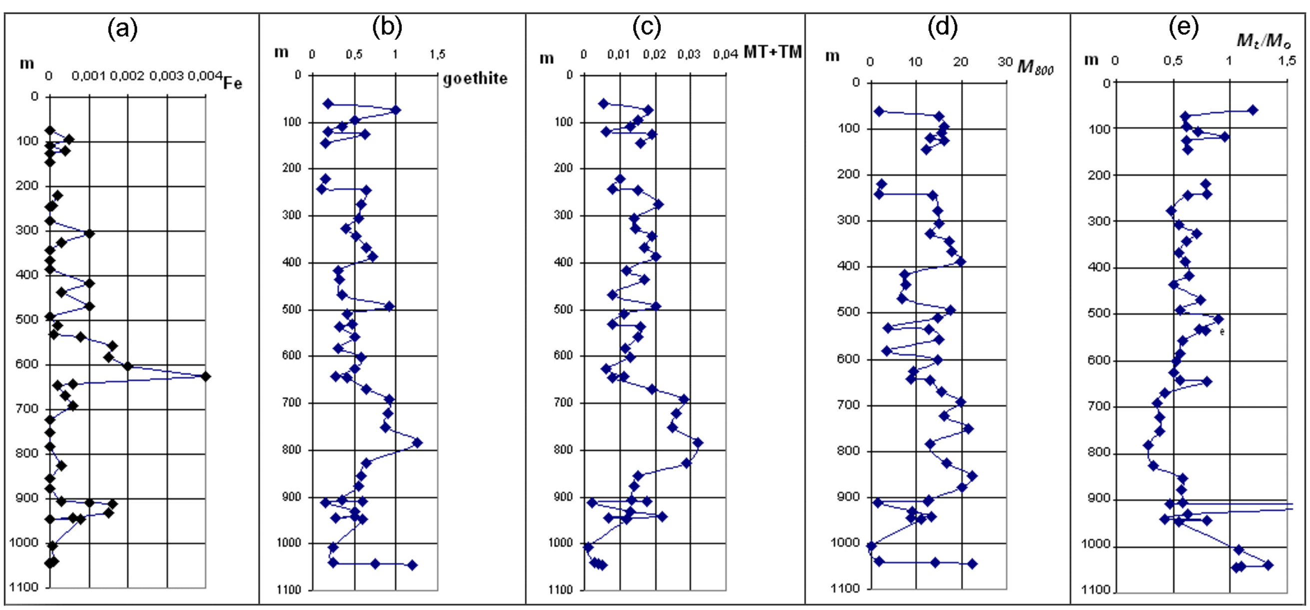

Figure 2. The distributions of (a) metallic iron (Fe), (b) goethite, (c) titanomagnetite+magnetite (TM+MT), (d) M_{800}, and (e) M_t/M_o, in the sediments of the Khalats section.

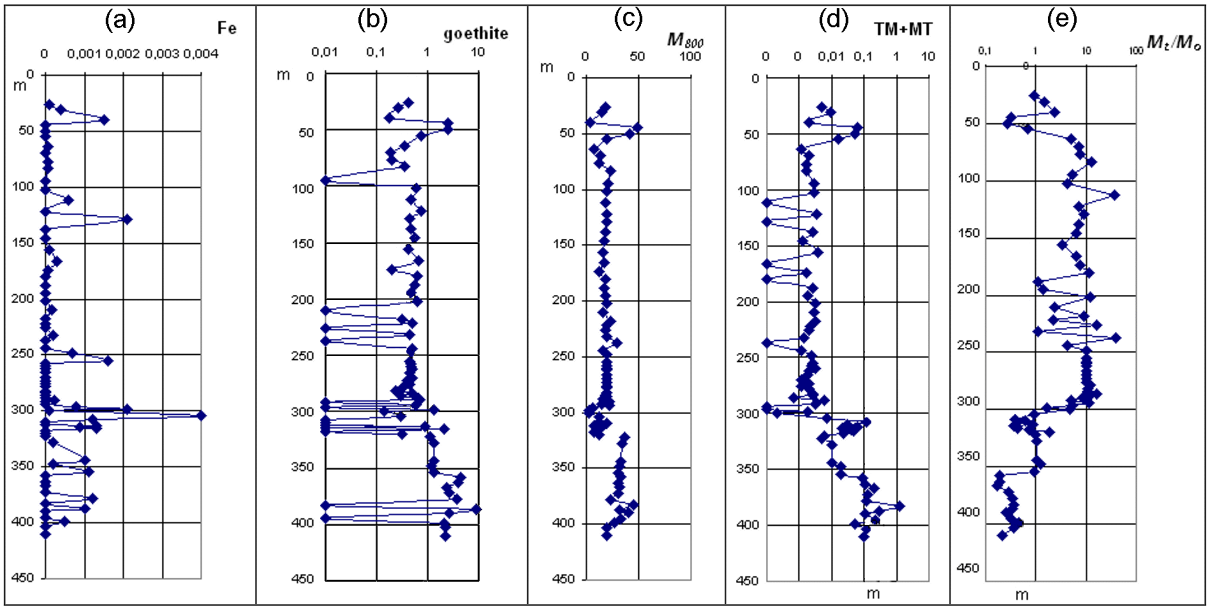

Figure 3. The distributions of (a) metallic iron (Fe), (b) goethite, (c) M_{800}, (d) titanomagnetite+magnetite (TM+MT), and (e) M_t/M_o, in the sediments of the Kvirinaki section.

of pyrite, which oxidizes into magnetite and hematite above 500°C [*Novakova and Gendler,* 1995].

[16] Let us now analyze the distribution of main magnetization carriers in the sediments of the Khalats and Kvirinaki sections.

[17] **Khalats.** The concentrations of Fe-hydroxides like goethite, magnetite+titanomagnetite and the total iron content as estimated by M_{800} value vary considerably along the section, partly repeating each other (Figure 2). The concentrations of magnetite+titanomagnetite and goethite correlate with M_t/M_o ratio (Figure 2b,c,e and Figure 4d,e); this correlation is negative, which points to a large contribution of maghemite and hence considerable low-temperature oxidation of magnetic minerals. The low-temperature oxidation zone is more distinct in the lower part of the section (700–820 m interval), where the concentrations of magnetite+titanomagnetite and goethite are higher (Figure 2b, c), and hematite is more common.

[18] The distribution of metallic iron looks dissimilar (Figure 2a): its concentration does not exceed 0.001%, and it is absent (more precisely, it is not detected by TMA). Two intervals with higher metallic iron content differ from this background: one with iron content up to 0.004% encompasses the 625–557 m part of the section (samples 38, 39, 41, and 42, Table 1, Figure 2a) and the second less clearly defined interval at 930–909 m with iron content up to 0.002% (samples 23, 24, and 25, Table 1, Figure 2a). According to correlation of paleomagnetic data from the Khalats section with geomagnetic polarity time scale, the upper iron-enriched interval covers the uppermost part of the C5Ar chron and about half of the C5An chron, i.e., about 12.6–12.2 Ma (Table 1). The lower iron-enriched interval is within a reverse subchron in the middle part of the C5Bn chron and hence is 15.2–15.0 Ma in age (Table 1).

[19] The similar variation in concentrations of goethite, magnetite+titanomagnetite, and M_{800} through the section is supported by significant correlations between these components (Figure 4). This is likely to indicate a similar terrestrial process of their accumulation. In contrast, the correlation between the above components and metallic iron is much weaker or absent altogether. This is mainly due to the large number of samples where metallic iron is not detected; a weak positive correlation, which is clearer for Fe-goethite (Figure 5a) and Fe-MT+TM (Figure 5b), is found in the remaining samples. Earlier in [*Pechersky,* 2008b], a significant positive correlation between cosmic metallic iron and goethite, magnetite, and titanomagnetite of definitely terrestrial origin, which has been found in many sedimentary sections from Europe and Asia, was accounted for by re-deposition of iron particles. This correlation is better visible for the logarithms of concentrations, and the logarithmic scale is used in the figures of this paper. As the zero value is absent in this data presentation, the value of 0.00001% (the lowest measurable concentration) was arbitrarily ascribed to the samples, for which no metallic iron was detected by TMA. It is worth stressing that a weak correlation in the Khalats sediments (Figure 5) indicates that metallic iron originated from both direct extraterrestrial input (cosmic dust and/or meteorites) and subsequent re-deposition. It is important that, as a rule, the highest values of metallic iron concentration do not fit the general trends (Figure 5).

[20] The Curie temperatures of iron particles are confined to a narrow range from 730°C to 770°C with a peak at 750°C, particularly, in the iron-enriched interval (Figure 6a). Hence the particles are composed of nearly pure iron with minor impurities.

[21] **Kvirinaki.** With respect to the Khalats section, magnetic minerals are more uniformly distributed in the

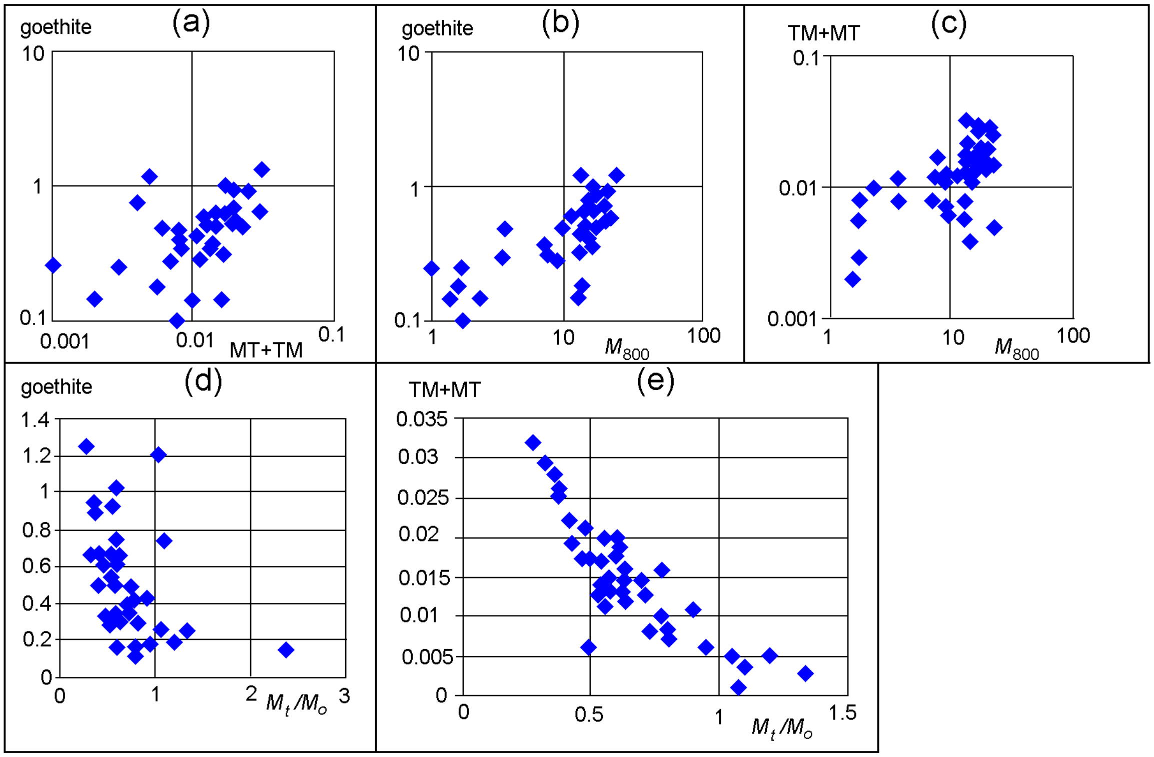

Figure 4. The correlation between the contents of goethite and magnetite+titanomagnetite (MT+TM) (a), goethite and M_{800} (b), titanomagnetite+magnetite (TM+MT) and M_{800} (c), goethite and M_t/M_o (d), titanomagnetite+magnetite (TM+MT) and M_t/M_o (e) in the Khalats sediments.

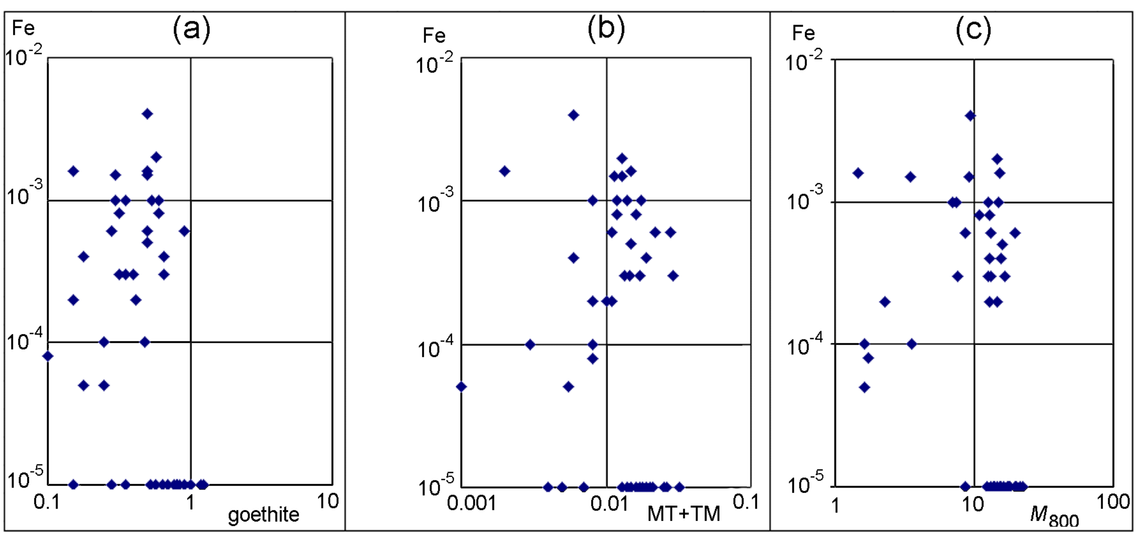

Figure 5. The correlation between the contents of metallic iron (Fe) and goethite (a), metallic iron (Fe) and titanomagnetite+magnetite (TM+MT) (b), metallic iron (Fe) and M_{800} (c), in the Khalats sediments.

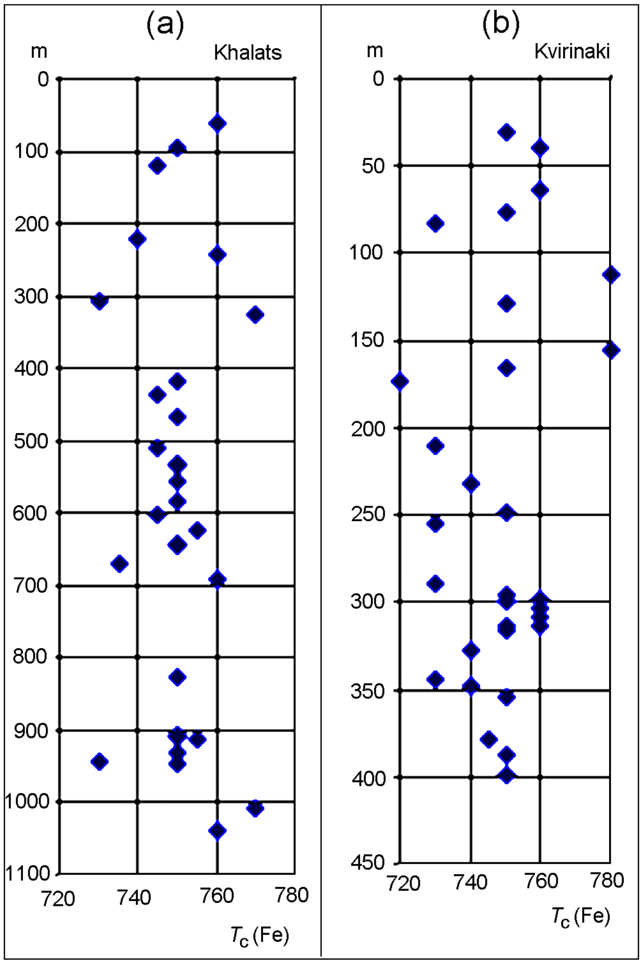

Figure 6. The distribution of Curie points of iron particles T_C(Fe) in the Khalats (a) and Kvirinaki (b) sections.

Kvirinaki section. Note also that the distributions of all magnetic components, metallic iron in particular, are different below and above the hiatus between 320 and 322 m (samples 390 and 391, Table 2, Figure 3). In the lower 100-meter part of the section below this large hiatus, the behavior of goethite, magnetite+titanomagnetite, and M_{800} is similar (Figure 3b,c,d). Similarly with the Khalats section, a zone of increased low-temperature oxidation, with the highest concentrations of goethite and magnetite+titanomagnetite and, correspondingly, the lowest M_t/M_o ratio values, is found at the base (350–400 m) of the Kvirinaki section (Figure 3b,d,e). The main difference between these two sections is the presence of pyrite over a large interval of the Kvirinaki sections. This is well manifested in TMA data by the growth of magnetization intensity and the M_t/M_o ratio above 500°C and is accounted for by transformation of pyrite into magnetite (Figures 1a, 3e). According to these data, pyrite is present in the 236 meter-thick interval out of the total thickness of 400 m. Pyrite is present at the interval, where the concentrations of other magnetic and paramagnetic minerals are very steady, while that of pyrite varies by an order of magnitude (Figure 3). We conclude that pyrite formation and preservation point to reducing environment of this part of the Kvirinaki section. The distribution of metallic iron particles clearly differs from those of other magnetic and paramagnetic components, but in general similarity is present too (Figure 3). In particular, somewhat elevated concentration of metallic iron, up to 0.001%, appears to be detected in the lower part of the section below the hiatus, that is where the concentrations of magnetic and paramagnetic minerals is elevated as well. In contrast, no iron is detected by TMA in the upper part of the section, where the concentrations of magnetic and paramagnetic minerals are relatively lower (Figure 3), and just three jumps of iron content up to 0.0015–0.002% are found (Figure 3a). An "anomalous" eighteen-meter thick interval that is relatively enriched, up to 0.004%, by metallic iron particles stands out from the general background (Figure 3a). According to magnetostratigraphic data, this interval covers the uppermost part of the chron C5Ar and about half of the C5An chron, i.e., from 12.6 to 12.2 Ma (Table 2, Figure 3a).

[22] Similarly to the Khalats data, a positive correlation exists between M_{800}, and the goethite and MT+TM concentrations (Figure 7), whereas no correlation is found for pyrite (Figure 7e). Note that the goethite content is perceptibly lower in the pyrite zone than outside of it (Figure 7e), which is likely due to oxidizing and reducing environment in these zones. It means that the origin and accumulation of magnetic minerals (most probably terrigenous) clearly differ from those of pyrite. The correlation between the above components and metallic iron is much weaker (Figure 8): it is virtually absent between iron and M_{800} (Figure 8c), or iron and pyrite (Figure 8d). Besides, metallic iron is absent altogether from many samples (Figure 8). Thus it is more likely that a considerable part of iron particles in sediments came directly from the cosmic dust and/or meteorites. On the other hand, the general patterns of separate minerals concentrations in this section that have been described above are similar, which is likely to indicate some re-deposition of iron particles. This is not related, however, for the narrow iron-enriched interval, which is certainly anomalous with respect to terrestrial minerals, like goethite, magnetite+titanomagnetite, pyrite, and paramagnetic iron compounds (M_{800}) (Figures 3 and 8). It is worth stressing that the iron-enriched interval straddles the maghemite and pyrite zones (Figure 3) and it thus independent of the redox conditions in sediments.

[23] The Curie temperatures of iron particles mainly range from 730°C to 770°C, with T_C = 760°C in the iron-enriched interval (Figure 6b). Hence the particles are composed of nearly pure iron with minor impurities.

Discussion

[24] It is important to illustrate the different lithological conditions of deposition, which may, or may not, affect the accumulation of metallic iron particles.

[25] 1) First of all, the steadily uniform concentrations of magnetic minerals in the Kvirinaki sediments point to unwavering regime of their accumulation, in contrast to more

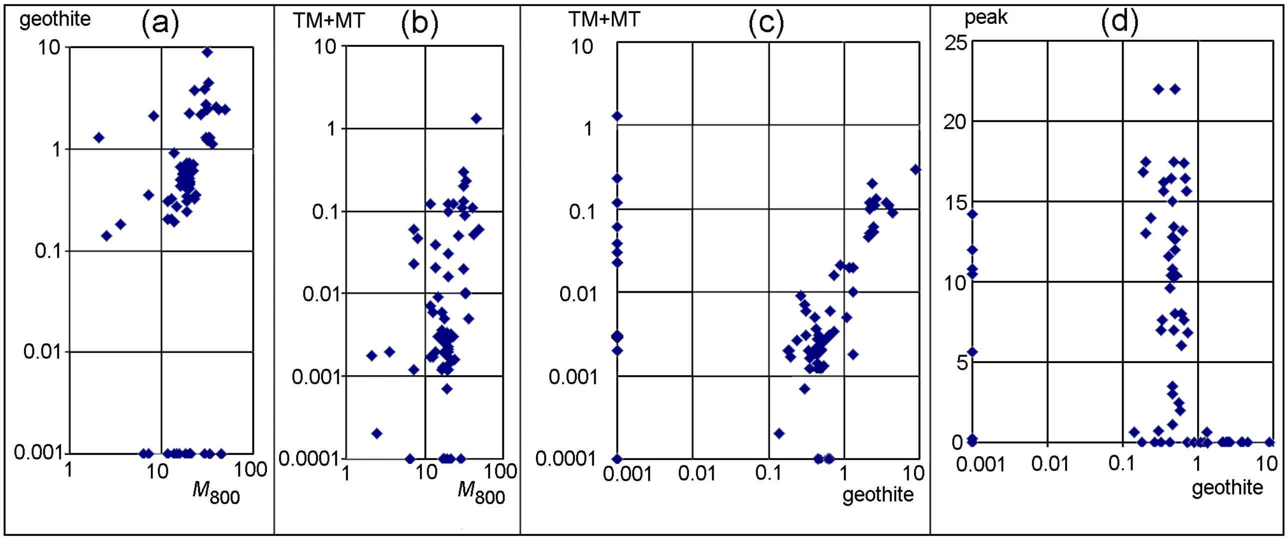

Figure 7. The correlation between the contents of goethite and M_{800} (a), titanomagnetite+magnetite (TM+MT) and M_{800} (b), titanomagnetite+magnetite (TM+MT) and goethite (c), goethite and the peaks on the $M_i(T)$ curves (d) in the Kvirinaki sediments.

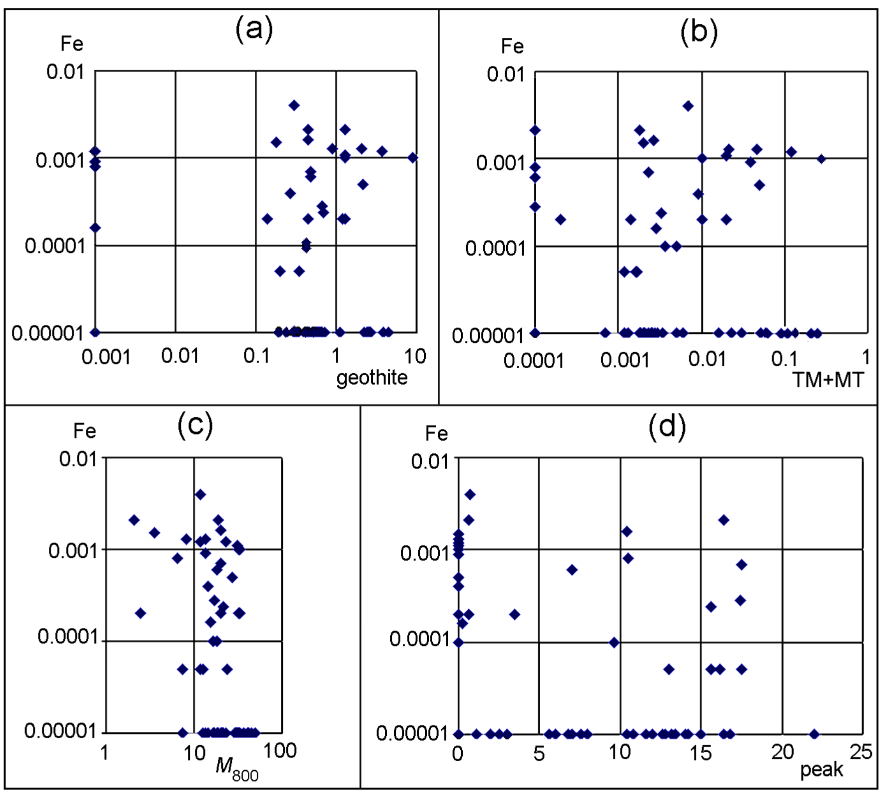

Figure 8. The correlation between the contents of metallic iron (Fe) and goethite (a), metallic iron (Fe) and titanomagnetite+magnetite (TM+MT) (b), metallic iron (Fe) and M_{800} (c), and metallic iron (Fe) and the peaks on the $M_i(T)$ curves (d) in the Kvirinaki sediments.

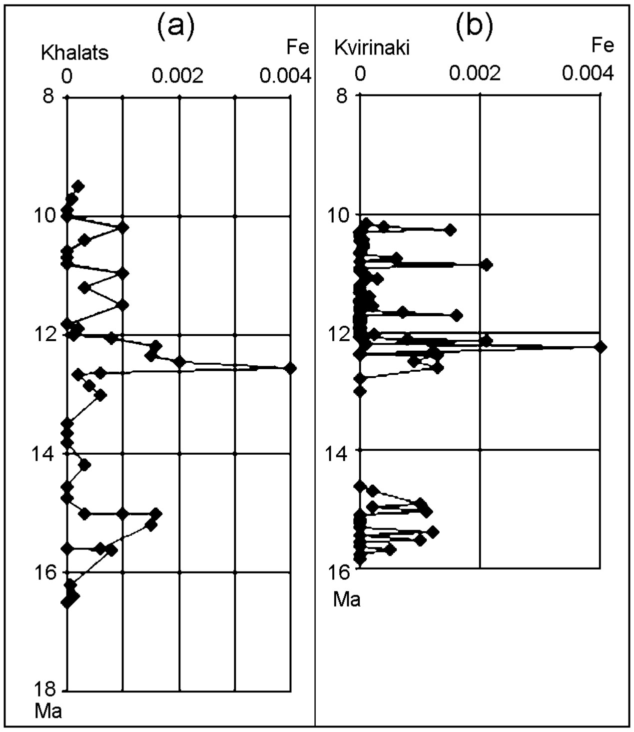

Figure 9. Time correlation of the Khalats (a) and Kvirinaki (b) sections.

variable accumulation of magnetic minerals in the Khalats deposits (Figures 2 and 3).

[26] 2) Pyrite is present in the upper part of the Kvirinaki section and is not found in the Khalats section altogether. Consequently, reducing conditions that govern the pyrite formation and preservation, prevailed over most the Kvirinaki sequence, with oxidizing conditions predominating at the base and the very top of the section and thus accounting for maghemitization of magnetite and titanomagnetite. In contrast, the nearly entire Khalats section is characterized by low-temperature oxidation of magnetite and titanomagnetite and maghemite formation. Hematite, which is not found in all the Kvirinaki samples, is present in many Khalats samples.

[27] 3) The magnetite+titanomagnetite content in the Kvirinaki sediments is generally higher than in the lower part of the Khalats section but is lower than in the upper part of the same section.

[28] 4) The base of the Kvirinaki section is perceptibly enriched by goethite (2–4%), while its concentration is less than 1–1.5% in the Khalats section. The upper parts of both sections contain about 0.5% of this mineral.

[29] 5) The lower part of the Kvirinaki section is relatively rich in paramagnetic iron compounds (M_{800} = 0.03–0.04 Am^2 kg^{-1}), whereas the upper part and the Khalats section contain lesser amounts of paramagnetic iron compounds, the values of M_{800} being ~0.02 Am^2 kg^{-1} and 0.005–0.02 Am^2 kg^{-1}, respectively.

[30] Therefore, the accumulation of iron particles superimposed on different backgrounds that are created by local physical-geographic peculiarities of deposition of coeval sediments. Note the only interval of relative enrichment (up to 0.004%) by metallic iron particles is recognized in both sections (Figures 2a and 3a). Judging by Curie temperatures of 750–760°C (Figure 6), the composition of iron particles is uniform and similar in both sections. According to magnetostratigraphic data, these iron-enriched intervals with ages of 12.6–12.15 My (Figures 9 and 10) are nearly synchronous. The positions of iron concentration maximums, however, are at the base of the interval (12.55 My) in the Khalats section and in the upper part of the interval in the Kvirinaki section (12.25 My). On the other hand, we cannot guarantee such a high precision of correlation. Secondly, even if the correlation is perfect, it is difficult to believe into the absolutely equal amounts of deposited iron particles over the distance of 1500 km. The latter was further tested in the following way: two additional samples were selected ~1 cm away from samples #38 and #41 with iron content of 0.004% and 0.0015%, respectively, from the Khalats collection; similarly, two more samples were taken close to the samples #395 (0.0013%) and #399 (0.004%) from the Kvirinaki collection. These additional samples, 38a (0.003%), 41a (0.002%), 395a (0.0019%) and 399a (0.0021%), reveal the elevated concentration of metallic iron too, the observed values being similar for the sister-samples. This indicates that the elevated concentration of metallic iron in the 12.6–12.15 My interval is real indeed, but the values themselves may vary from 0.002 to 0.004% even for the same stratigraphic level. So it is not surprising that these values vary over 1500 km.

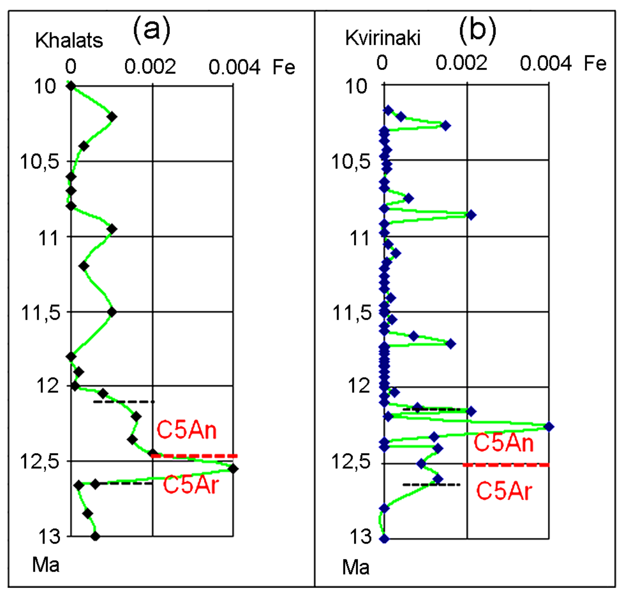

Figure 10. The comparison of the intervals of elevated concentrations of metallic iron particles for the Khalats (a) and Kvirinaki (b) sections on the expanded scale. Black horizontal dashed lines denote the boundaries of the metallic iron content of ≥0.001%; red horizontal solid lines stand for the boundaries of the C5Ar and C5An magnetic chrons.

[31] It is interesting that three narrow maximums of iron content of 0.001–0.002% in the upper parts of both sections are also synchronous within the error limits, the ages of these maximums being 10.2, 10.95, and 11.5 My for the Khalats section and 10.26 Ma, 10.85 Ma, and 11.7 My for the Kvirinaki section (Figure 10). These maximums are found in the sediments that accumulated under very different conditions, i.e., oxidizing in the Khalats section and reducing in the Kvirinaki section.

[32] The above correlation of iron-enriched intervals in sediments from remote sections indicates a global event of cosmic iron precipitation on the Earth at these times. Judging by the duration of 0.4 My of the main iron-enriched interval, it cannot have resulted from a single, whatever huge, impact event but had to be a series of global synchronous events or an a prolonged process.

[33] The long hiatus that is present in the Kvirinaki section is entirely overlapped in the Khalats one (Figure 9). As testified by these data, no perceptible events of iron particles precipitation occurred during the 14.6–13 Ma interval. Before that, a detectable amount of iron particles is found in the Kvirinaki area in the 15.6–14.9 Ma interval; their concentration reaches 0.001%, with the a gap between 15.3 and 15.1 Ma, where no metallic iron is found. This no-iron interval (15.2–15.0 Ma) coincides with elevated iron concentration of 0.0016% in the Khalats area (Figure 9). This misfits that are also found for the peaks in the 12–10 Ma interval, can be attributed to inaccuracies in dating, to imperfect correlation between the sections and geomagnetic polarity time scale, and, finally, to the impression of the scale itself.

Conclusions

[34] With the aid of thermomagnetic analysis up to 800°C we revealed the detailed pattern of how metallic iron particles are distributed in space and time, which is impossible to detect with "direct methods". Our main discovery is the synchronous enrichment by iron particles in Miocene sediments of the Khalats and Kvirinaki sections that are more than 1500 km apart. This phenomenon that occurred 12.6–12.2 Ma, is most likely to be global and space-connected. It does not depend upon local deposition, sediment composition, redox conditions, etc. Long duration of this phenomenon and its global scale cannot have resulted from a single impact event.

References

Berggren, W. A., D. V. Kent, C. C. Swisher III, and M. Aubry (1995), A revised Cenozoic geochronology and chronostratigraphy, Geochronology Time Scale and Global stratigraphic Correlation, *Society for Sedimentary Geology (SEPM), Special Publication,* no. 54, 129.

Burov, B. V., D. C. Nourgaliev, and P. G. Yasonov (1986), *Paleomagnetic Analysis* (in Russian), 167 pp., Kazan State University, Kazan.

Grachev, A. F., O. A. Korchagin, H. Kollmann, D. Pechersky, and V. Tselmovich (2005), A new look at the nature of the transitional layer at the K/T boundary near Gams, Eastern Alps, Austria, and the problem of the mass extinction of the biota, *Russ. J. Earth Sci., 7,* ES6001, doi:10.2205/2005ES000189.

Molostovsky, E. A., V. A. Fomin, and D. M. Pechersky (2006), Sedimentogenesis in Maastrichtian-Danian basins of the Russian plate and adjacent areas in the context of plume geodynamics, *Russ. J. Earth Sci., 8,* ES6001, doi:10.2205/2006ES000206.

Novakova, A. A., and T. Gendler (1995), Metastable structural-magnetic transformations in sulfides in course of oxidation, *J. Radioanal. Nucl. Chem., 190*(2), 363.

Pechersky, D. M. (2008a), Enrichment of sediments by Fe-hydroxides at the Mesozoic-Cenozoic boundary: A compilation rock-magnetic data, *Izv. Phys. Solid Earth,* no. 3, 65.

Pechersky, D. M. (2008b), Metallic iron in sediments at K/T boundary, *Russ. J. Earth Sci., 9,* 1.

Pechersky, D. M., A. F. Grachev, D. Nourgaliev, V. Tselmovich, and Z. Sharonova (2006a), Magnetolithologic and magnetomineralogical characteristics of deposits at the Mesozoic/Cenozoic boundary: Gams section (Austria), *Russ. J. Earth Sci., 8*(3), ES3001, doi:10.2205/2006ES000204.

Pechersky, D. M., D. K. Nurgaliev, and Z. Sharonova (2006b), Magnetolithologic and magnetomineralogical characteristics of deposits at the Mesozoic/Cenozoic boundary: Koshak section (Mangyshlak), *Izv. Phys. Solid Earth,* no. 10, 99.

Rochette, P., M. Jackson, and C. Aubourg (1992), Rock magnetism and interpretation of anisotropy of magnetic susceptibility, *Reviews of Geophysics, 30,* 209.

D. K. Nurgaliev, Geological Faculty, Kazan State University, 18 Kremlevskaya, 420008 Kazan, Tatarstan, Russia (danis.nourgaliev@ksu.ru)

D. M. Pechersky, Schmidt Institute of Physics of the Earth, Russian Academy of Sciences, 10 B. Gruzinskaya, 123995 Moscow, Russia

V. M. Trubikhin, Geological Institute, Russian Academy of Sciences, 7 Pyzhevsky lane, 119017 Moscow, Russia